Front. Earth Sci. 2024, 18(3): 637–648
https://doi.org/10.1007/s11707-024-1107-0

RESEARCH ARTICLE

The characteristics and future projections of fire danger in the areas around mega-city based on meteorological data–a case study of Beijing

Mengxin BAI[1], Wupeng DU (✉)[1], Zhixin HAO[2,3], Liang ZHANG[2,3], Pei XING[1]

1 Beijing Municipal Climate Center, Beijing Meteorological Service, Beijing 100089, China
2 Key Laboratory of Land Surface Pattern and Simulation, Institute of Geographic Sciences and Natural Resources Research, Chinese Academy of Sciences, Beijing 100101, China
3 University of Chinese Academy of Sciences, Beijing 100049, China

Abstract It is crucial to investigate the characteristics of fire danger in the areas around Beijing to increase the accuracy of fire danger monitoring, forecasting, and management. Using meteorological data from 17 national meteorological stations in the areas around Beijing from 1981–2021, this study calculated the fire weather index (FWI) and analyzed its spatiotemporal characteristics. It was found that the high and low fire danger periods were in April–May and July–August, with spatial patterns of "decrease in the northwest–increase in the southeast" and a significant increase throughout the areas around Beijing, respectively. Next, the contributions of different meteorological factors were quantified by the multiple regression method. We found that during the high fire danger period, the northern and southern parts were affected by precipitation and minimum relative humidity, respectively. However, most areas were influenced by wind speed during the low fire danger period. Finally, comparing with the FWI characteristics under different SSP scenarios, we found that the FWI decreased during high fire danger period and increased during low fire danger period under different SSP scenarios (i.e., SSP245, SSP585) for periods of 2021–2050, 2071–2100, 2021–2100, except for SSP245 in 2071–2100 with an increasing trend both in high and low fire danger periods. This study implies that there is a higher probability of FWI in the low fire danger period, threatening the ecological environment and human health. Therefore, it is necessary to enhance research on fire danger during the low fire danger period to improve the ability to predict summer fire danger.

Received February 22, 2023; accepted October 24, 2023

E-mail: duwupeng@sina.com

Keywords meteorological data-based fire danger, areas around Beijing, climate characteristics, SSP scenarios

1 Introduction

Fire danger is one of the most significant natural disturbance processes in the global ecosystem and a critical natural hazard to forests, grasslands, cropland, etc. (McDowell and Allen, 2015; de Sousa et al., 2022). For instance, the average number of fires per year from 2005 to 2015 was above 70,000, with a total deforestation area of 6.7×10^8 hm^2, which resulted in direct economic losses of hundreds of billions of dollars (Esperson-Rodriguez et al., 2022). Fire dangers are one of the important drivers of global climate change by destroying surface vegetation and releasing large amounts of greenhouse gases and particulate matter (Justino et al., 2011; Kelly et al., 2020). It is crucial that vegetation has a significant role in mitigating global warming while also providing environmental services and socioeconomic benefits to people (Guidolotti et al., 2017; Pataki et al., 2021; Richards et al., 2022). This involves two key processes: 1) limiting sunlight to create a cooling effect and 2) using carbon capture and sequestration to significantly contribute to reaching forest carbon neutrality and carbon peaking (Hardiman et al., 2017; Ibsen et al., 2021; Wei et al., 2021). This demonstrates that the development of forests in the areas around mega-city is a very important pathway to address the impact of climate change. As a result, the current research on fire dangers is extremely valuable given the ongoing growth of forests in the areas around mega-city.

Beijing, the capital of China and one of the world's mega-cities, had a resident population of 21.88 million in

2021. The ecological needs of such a large city are severe. The western and northern parts of the Beijing area are located in the Taihang Mountains and Yanshan Mountains, respectively. Mountainous areas accounted for approximately 62% of the total area of Beijing, with high forest cover in the west and north (Xie et al., 2010; Zhang et al., 2011). Beijing began the first phase of its "million ha afforestation project" in 2012, putting an end to the ecological condition known as "city without forest" in Beijing. Another phase of afforestation work started in 2018, and as of this year, 1.01 million ha of land had been covered in trees. Additionally, the areas around Beijing have also created the "Ecological Conservation Zone", which is primarily focused on developing ecological conservation mechanisms and ecological management capabilities, driving regional economic development with cultural tourism, ecological civilization, and other industrial development, while improving the quantity and quality of ecological resources (Cheng et al., 2020). This was done to meet the demand for urban ecology from the public. Beijing's climate is controlled by both the East Asian monsoon system and the western part of the western Pacific Ocean, which results in complex climate characteristics (Ding et al., 2008, 2009). According to the Beijing Emergency Management Bureau, a total of 43 fires occurred in the areas around Beijing between 2016 and 2019 due to climatic conditions which caused serious impacts. Therefore, it is imperative that we understand the spatiotemporal characteristics of fire danger in the areas around Beijing and its potential causes. This knowledge is important for the advancement of sophisticated monitoring and forecasting techniques for the forest fire danger of areas around Beijing in the future.

However, most current studies on fire dangers have focused on winter and spring, when low precipitation and high wind speed provide favorable climatic conditions for fire danger to occur. Our knowledge of fire danger variations in other seasons is still unclear, especially in summer. Fire danger occurring in summer causes irreversible effects on forests. For example, fires in Australia from 2019/12 to 2022/2 lasted three months throughout the summer, killing 33 people and 3 billion animals and causing damage of close to $50 million (Nolan et al., 2020; Ward et al., 2020; Squire et al., 2021; Cai et al., 2022). In August 2022, fires persisted nationwide due to the persistently high temperatures and drought in southern China, notably the mountain fires in Chongqing that lasted for three days and severely disrupted local human and material livelihoods. Increased sensitivity of fire danger to high temperatures in the context of global warming, has led to longer meteorological fire danger periods and drying of combustible material (increased evapotranspiration and drying of deadfall), which triggered the occurrence of more meteorological risks of forest fires (Flannigan et al., 2009; Jolly et al., 2015; Jain et al., 2022). Meanwhile, the impact of human activities, such as large greenhouse gas emissions and land use/cover changes, has led to increased frequency of extreme weather and climate events through processes such as altered land-air interactions and sea-air interactions, which in turn affected the length of fire danger periods and fire intensity, etc. (Kloster et al., 2012; Zou et al., 2021; Ying et al., 2022). Some studies showed that the average annual fire area in the western United States was expected to increase by 54% by the 2050s, and the fire area in the North-west Pacific and Rocky Mountain forests will increase by 78% and 175%, respectively, in the context of the future climate change (Spracklen et al., 2009). Meanwhile, the number of meteorological fires in north China will increase by 30% by 2030. Potential fires in north-east China will increase by 10% to 18% from 2071 to 2100, and the fire danger period will be extended by 21 to 26 days (Tian et al., 2011). Therefore, it is urgently necessary to strengthen the analysis of the spatiotemporal characteristics of fire dangers in the summer season, as well as to predict the spatial pattern of fire danger in the areas around Beijing under various Shared Socioeconomic Pathway (SSP) scenarios in the future in the context of frequent extreme temperature and drought. This is crucial to prevent fire dangers.

Herein, this study aims to explore the spatiotemporal variation in fire danger in the areas around Beijing and future projections. This study addresses the following questions. 1) What are the spatiotemporal patterns of fire danger in the areas around Beijing over the past 40 years and the primary influencing factors? 2) What are the spatial patterns of fire danger in the areas around Beijing under different SSP scenarios?

2 Materials and methods

2.1 Study area

The Beijing area is located in the north-western portion of the North China Plain, ranging from 115.38°E–117.50°E and 39.43°N–41.05°N (Fig. 1). The study area has a monsoon climate zone that is characterized by cold, dry winters and hot, rainy summers. The average annual temperature is approximately 10°C–13°C, and the total annual precipitation is approximately 600 mm. However, the seasonal distribution of precipitation is uneven, with summer precipitation predominating due to the East Asia Summer Monsoon (Jia et al., 2017). Additionally, the western and northern parts of the Beijing area are located in the Taihang and Yanshan Mountains, respectively. The mountainous area accounts for approximately 62% of the total area of Beijing, with high forest cover in the west and north, as well as some grassland in the north and southwest. The vegetation type is warm-temperate,

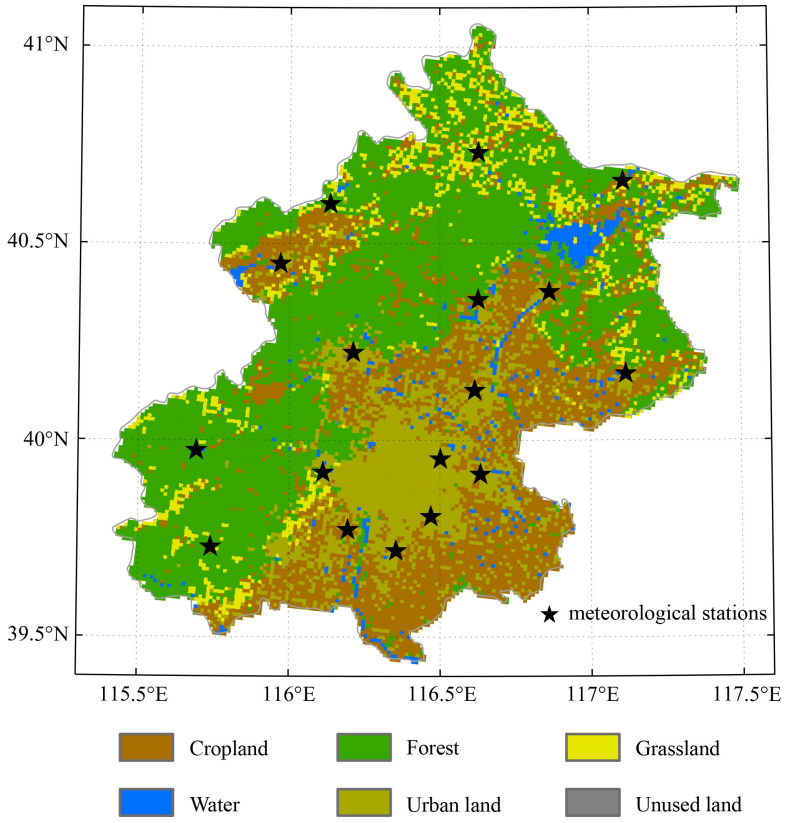

Fig. 1 Land use in 2015 in Beijing areas and the locations of 17 national meteorological stations in the areas around Beijing.

deciduous broad-leaved forest interspersed with temperate coniferous forest. The abovementioned land types are highly vulnerable to high temperatures and drought, which could trigger fire dangers and disrupt the ecological balance. Moreover, there are partially forest and grassland in suburb areas (Xie et al., 2010).

2.2 Data

The daily average meteorological observations from 17 national stations in the areas around Beijing, including maximum surface air temperature (T_{max}) at 2 m and precipitation, minimum relative humidity (RH_{min}), and wind speed at 10 m during 1981−2021, were obtained from the Beijing Meteorological Information Center. These 17 national meteorological stations were not located in urban land. The data set was subjected to strict quality control, such as removing outliers and homogenizing data due to meteorological station relocation or meteorological instrument replacement.

The daily simulation data, including T_{max} at 2 m and precipitation, RH_{min}, and wind speed at 10 m, were derived from nine global climate models (Table 1) involved in Coupled Model Intercomparison Project Phase 6 (CMIP6) in this study. Moreover, three sets of experiments, including historical simulation, SSP245, and SSP585 scenario simulations, were employed. The historical simulations used real-time, dynamic external forcing of volcanic aerosols, solar irradiation, greenhouse gases (GHGs), and land use/cover change (LUCC) (Taylor et al., 2012). Therefore, full-forcing experiments represent climate change driven by both external forcing and internal variability. SSP245 and SSP585 reflect a set of alternative future scenarios of social development and greenhouse gas emissions. SSP245 represents the combined scenario of a moderate socioeconomic development path (i.e., SSP2) with medium-low radiation forcing, which peaks at 4.5 $W \cdot m^{-2}$ by 2100. SSP585 represents the combined scenario of a high energy-intensive, socioeconomic developmental path (i.e., SSP5) with strong radiative forcing, which peaks at 8.5 $W \cdot m^{-2}$ by 2100 (O'Neill et al., 2016; Riahi et al., 2017).

2.3 Methods

2.3.1 Fire Weather Index

The fire weather index (FWI) is based on the time-lag-equilibrium water content theory, which organically relates meteorological conditions and combustible water content (Wagner, 1987). This index is widely used in many countries worldwide (Amiro et al., 2004; de Groot et al., 2007). Notably, Tian et al. (2006) demonstrated that the FWI applies to fire danger assessment in the areas around Beijing.

The FWI system consists of six indices, including the

Table 1 The information of CMIP6 models used in this study

ID	Model name	Institution and region	Atmospheric resolution (lon × lat, vertical levels)
1	ACCESS-ESM1-5	Commonwealth Scientific and Industrial Research Organization, Australia	~1.88° × 1.25°, L38
2	CanESM5	Canadian Centre for Climate Modeling and Analysis, Canada	~2.81° × ~2.77°, L49
3	CMCC-ESM2	Euro-Mediterranean Centre for Climate Change Foundation, Italy	1.25° × ~0.94°, L30
4	EC-Earth3	EC-Earth Consortium, Europe	~0.71° × ~0.70°, L91
5	FGOALS-g3	Chinese Academy of Sciences, China	2° × ~5.18°, L26
6	GFDL-CM4	National Oceanic and Atmospheric Administration, Geophysical Fluid Dynamics Laboratory, USA	1.25° × 1°, L33
7	INM-CM5-0	Institute for Numerical Mathematics, Russia	2° × 1.5°, L73
8	MIROC6	Atmosphere and Ocean Research Institute, The University of Tokyo, Japan	~1.41° × ~1.39°, L81
9	MPI-ESM1-2-LR	Max Planck Institute for Meteorology, Alfred Wegener Institute, Germany	~1.88° × ~1.85°, L47
10	MRI-ESM2-0	Meteorological Research Institute, Japan	~1.13° × ~1.11, L80

fine fuel moisture code (FFMC), duff moisture code (DMC), drought code (DC), initial spread index (ISI), build-up index (BUI), and FWI. The inputs of the FWI system are daily meteorological data, including T_{max} at 2 m and precipitation, RH_{min}, and wind speed at 10 m.

Notably, the calculation of cumulative relative humidity and temperature is involved in the FWI. Therefore, it was deemed in this study that calculation results of the initial state could not be employed. So, we first used daily observation data from 1981–2021 to calculate the daily FWI. Next, we used the daily FWI to calculate its monthly average to obtain the monthly scale FWI in this study. Finally, we employed the monthly FWI from 1982–2021 to analyze fire danger characteristics and the difference between high and low fire danger periods. Similarly, we used daily simulated data from 2020 to 2100 to construct the daily FWI and calculate its monthly average FWI regarding FWI climatology. Additionally, we analyzed the monthly FWI from 2021 to 2100.

2.3.2 Contribution of meteorological factors to the FWI

We calculated the contribution of each meteorological factor to the FWI to quantitatively assess their effect. We constructed the regression equation based on four meteorological factors (i.e., T_{max} and precipitation, RH_{min}, and wind speed) and FWI using the multiple linear regression approach. By dividing each regression coefficient's absolute value by the total of all coefficients' absolute values, the contribution of each meteorological component was calculated.

2.3.3 Taylor diagram and spatial interpolation

A Taylor diagram was used to evaluate whether the simulated-based FWI in climate models over the areas around Beijing could reproduce the characteristics of observational-based FWI. This diagram provided a concise statistical summary of how well a simulated pattern matched an observed pattern in terms of the spatial correlation coefficient (SCC), the root-mean-square error (RMSE), and the normalized standard deviations (NSD).

Considering the differences in spatial resolution among different models, this study first employed a bilinear interpolation algorithm to uniformly interpolate all modes to 0.25° × 0.25°. Then, we calculated a multi-model ensemble mean (MME) for all models. Finally, we utilized the results of MME to analyze the spatial patterns of FWI trends.

3 Results

3.1 Temporal variations in meteorological observation-based FWI

Figure 2 shows the monthly scale average of the FWI variations at 17 national meteorological stations in the areas around Beijing during 1982–2021. We found that the range of the FWI was from 5.56 to 32.15. There were significant intra-annual oscillations in one year for the FWI, exhibiting a peak and a valley. In detail, the average FWI in spring (i.e., April and May) was the highest, reaching 28.02. The average FWI in summer (i.e., July

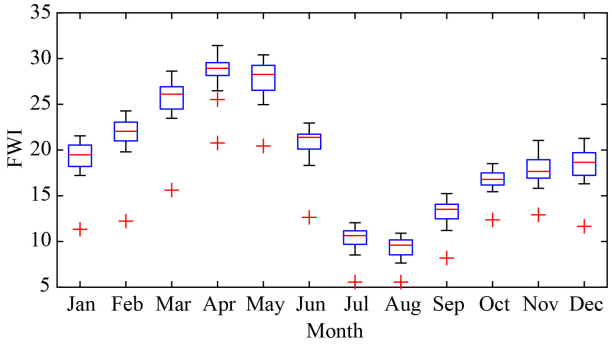

Fig. 2 Monthly average FWI variation in the areas around Beijing.

and August) was the lowest, less than 9.79. The FWI values in the other seasons were similar, especially in late fall and early winter.

Meanwhile, compared with the other 16 stations, we found a relatively small outlier FWI value in each month for one national meteorological station: Foyeding. Notably, its intensity for each month was twice as small as the average FWI of other stations. This may be due to the higher elevation of the Foyeding station, which exceeds 1200 m, while other stations are only approximately 29.6−489.4 m. In general, as altitude increased, temperature and relative humidity decreased, while wind speed increased. Therefore, the FWI value of the Foyeding station was smaller than that of the other stations. Although the FWI values varied among the 17 stations, they were all equally characterized by significant intra-annual oscillations with one peak in spring and a valley in summer. Therefore, we defined April–May as the high fire danger period and July–August as the low fire danger period in this study. Moreover, we further compared the characteristics and projections of the FWI for the high and low fire danger periods.

3.2 Spatial patterns of meteorological observation-based FWI

Figure 3 illustrates that the FWI trend for the high fire danger period displayed a north-western decrease and south-eastern increase in Beijing. The FWI tended to decrease in the area west of the boundary, with a declining rate that ranged from 0.58/(10 yr) to −0.13/(10 yr). In detail, the highest declining rates, up to an average of −0.54/(10 yr), were recorded at the Yanqing and Foyeding stations in western Beijing. However, there was an increasing trend of the FWI east of the boundary at a rate of 0.13/(10 yr) to 1.65/(10 yr). The Xiayunling station in the south-west and Fangshan station in the south had the greatest increases in fire danger. The trends of the FWI at all stations were noticeably higher during low fire danger periods with significance at a confidence level of 0.05. Particularly, the south had the most propensity for the FWI to rise, with values between 1.51 and 1.86. The increase in stations around the urban area was also very obvious. The ecological environment, vegetation phenology, and biodiversity may be substantially impacted by the heightened fire danger in summer in areas such as forests and cropland, seriously damaging ecological conservation areas and interfering with human tourism activities, etc.

The above-mentioned results indicated that the FWI in Beijing exhibited a spatial pattern of a “decreasing trend in the northwest and increasing trend in the southeast” during the high fire danger period. The FWI of the whole Beijing area had a trend of large-scale considerable increase during the low fire danger period. Moreover, the Beijing areas suffered a significant risk in the low fire danger season compared to the high fire danger period. The previously considered low fire danger period, summer, had seen a rapid increase rate of the FWI during this period under global warming, which could be irreversibly destructive to dense local vegetation and arable land in the middle of harvest. It is possible that summer fire danger threats will be more widespread and intense than spring fire threats because human knowledge of fire danger monitoring in summer is still insufficient. Therefore, we must deploy monitoring of summer fire danger sites as soon as possible to avoid severe risks. As mentioned in reports, local human safety and property security have all suffered irreparable harm as a result of the persistently high temperatures and drought that occurred in Australia’s summer of 2019/12–2020/2 and in southern China’s summer of 2022 (Nolan et al., 2020;

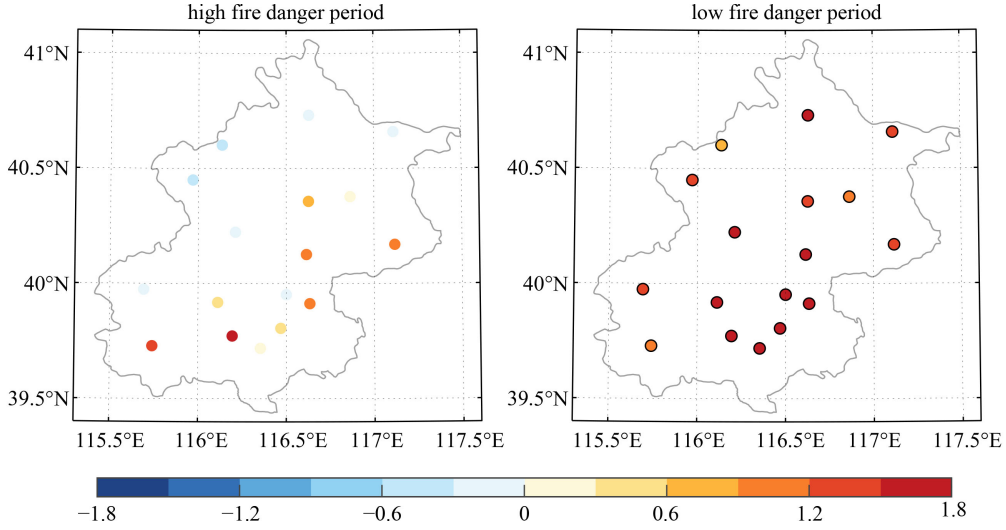

Fig. 3 Spatial patterns of the FWI trends in the areas around Beijing from 1982 to 2021 (units: (10 yr)$^{-1}$; the black circles denote significance at a confidence level of 0.05).

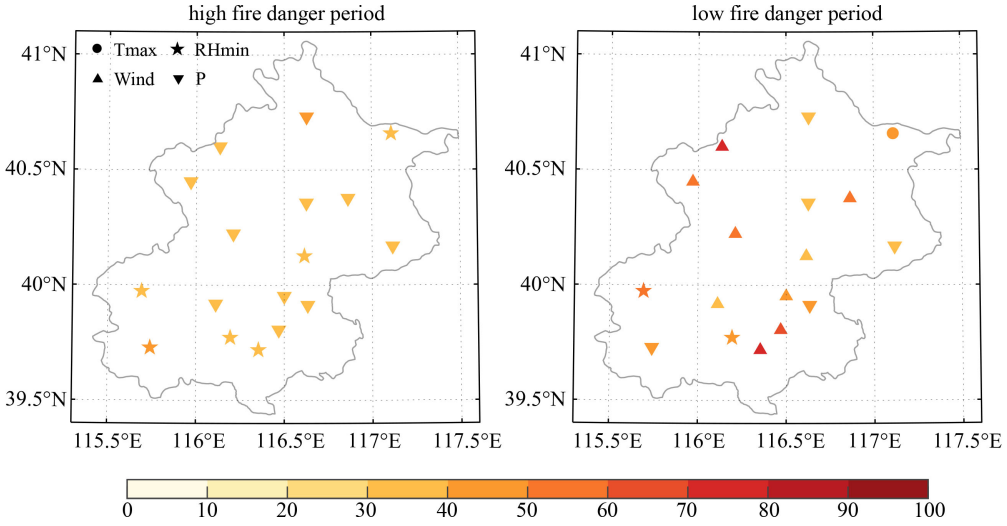

Fig. 4 Contribution rate of first contribution meteorological factor for FWI in Beijing during 1982–2021 (units: %).

Ward et al., 2020; Squire et al., 2021; Cai et al., 2022; Global Times, 2022). The frequency of summer fire hazards in recent years has also served as confirmation of the significance of summer fire danger monitoring.

The primary meteorological factor affecting the FWI in the high/low fire danger period is depicted in Fig. 4. During 1982–2021, precipitation had the greatest impact on the decreases in the FWI for the high fire danger period in northern and western Beijing, which may be caused by a significant increase in spring precipitation in the above-mentioned areas. However, the increases in the FWI in western and southern Beijing were mainly influenced by the minimum relative humidity. The decrease in minimum relative humidity over the past 40 years was not conducive to fire danger. It is noted that the average value of the most significant meteorological factor contribution rate was approximately 26%, and the maximum value did not exceed 30%.

In the low fire danger period, the enhancements of widespread fire danger across Beijing were influenced by different meteorological factors, including T_{max}, precipitation, wind speed, and RH_{min}. Most areas were mainly affected by wind speed variations. The contribution rate generally exceeded 30% and reached more than 75% in some areas, suggesting that the effect of summer wind speed on the FWI during the low fire danger period was relatively stable. The increase in wind speed in Beijing significantly enhanced the local fire danger, especially in the northwestern and southern parts. In addition, individual stations in the north were affected by

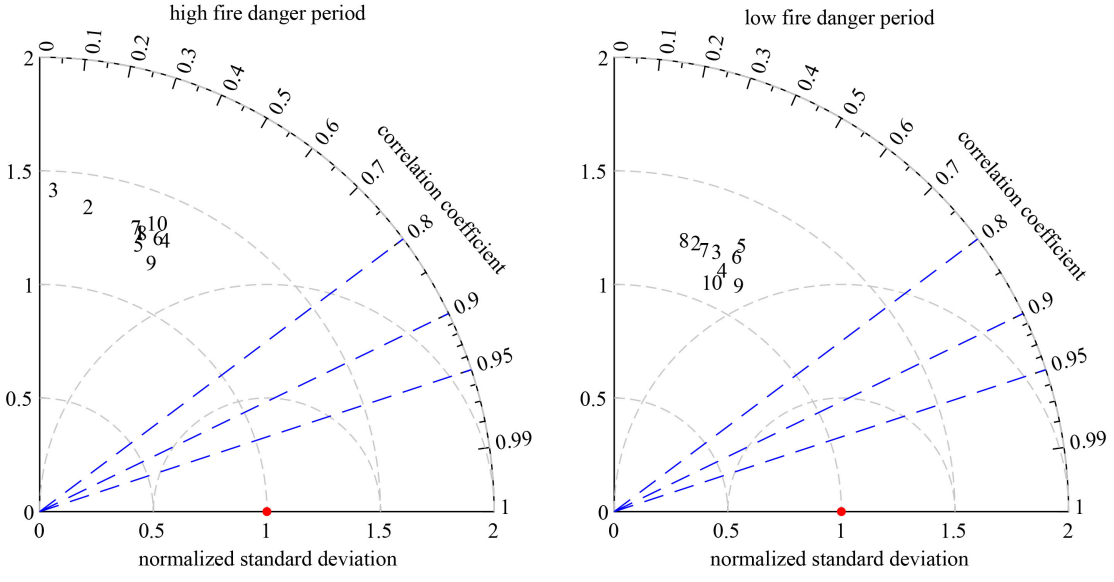

Fig. 5 Taylor diagram of simulating capability for the fire weather index during 1982–2021 (1: ACCESS-ESM1-5; 2: CanESM5; 3: CMCC-ESM2; 4: EC-Earth3; 5: FGOALS-g3; 6: GFDL-CM4; 7: INM-CM5-0; 8: MIROC6; 9: MPI-ESM1-2-LR; 10: MRI-ESM2-0).

precipitation, leading to enhanced fire danger.

These results indicated that the meteorological factor variations in different seasons have an inconsistent impact on the FWI. Changes in precipitation and RH_{min} have a major impact on the FWI during high fire danger periods, whereas wind speed has a major impact on the FWI during low fire danger periods. Therefore, different seasons need to focus on monitoring different types of meteorological factors to prevent forest fires.

3.3 Evaluation of CMIP6 models in simulating FWI

To assess the ability of the CMIP6 models to simulate the FWI, Taylor diagrams were drawn for the simulated FWI in the Beijing region (Fig. 5). From the spatial correlation coefficient perspective, all models were between 0.35 and 0.5 in the high fire danger period, except for models 2 (CanESM5) and 3 (CMCC-ESM2). Meanwhile, the ranges of normalized standard deviation of all models from observations were 1.15 to 1.45. In general, the simulation abilities of models 1 and 4−10 were comparable, and they all could reasonably reproduce the spatial distribution of the FWI during the high fire danger period. The spatial correlation coefficients of all models ranged from 0.25 to 0.5 in the low fire danger period, and the normalized standard deviations were 1−1.4. The capabilities of all ten models were similar.

These above-mentioned results suggested that except for models 2 and 3, the other model simulation performances were close, and they could better reproduce the spatial correlation of the FWI of the Beijing area during the high/low fire danger period. Consequently, the spatiotemporal characteristics under the different SSP scenarios were examined by the MME of eight climate models, including models 1, 4−10, in the following sections.

3.4 Characteristics of CMIP6 simulation-based FWI under SSP scenarios

In the context of the moderate emission scenario (SSP245), the spatial pattern of the FWI in Beijing during the high fire danger period showed a decreasing trend in 2021−2100, and its decreasing trend gradually increased from north to south. However, the FWI displayed an increasing trend that gradually spread from east to the west in the low fire danger period (Fig. 6). In detail, the north exhibited the slightest decreasing trend, only

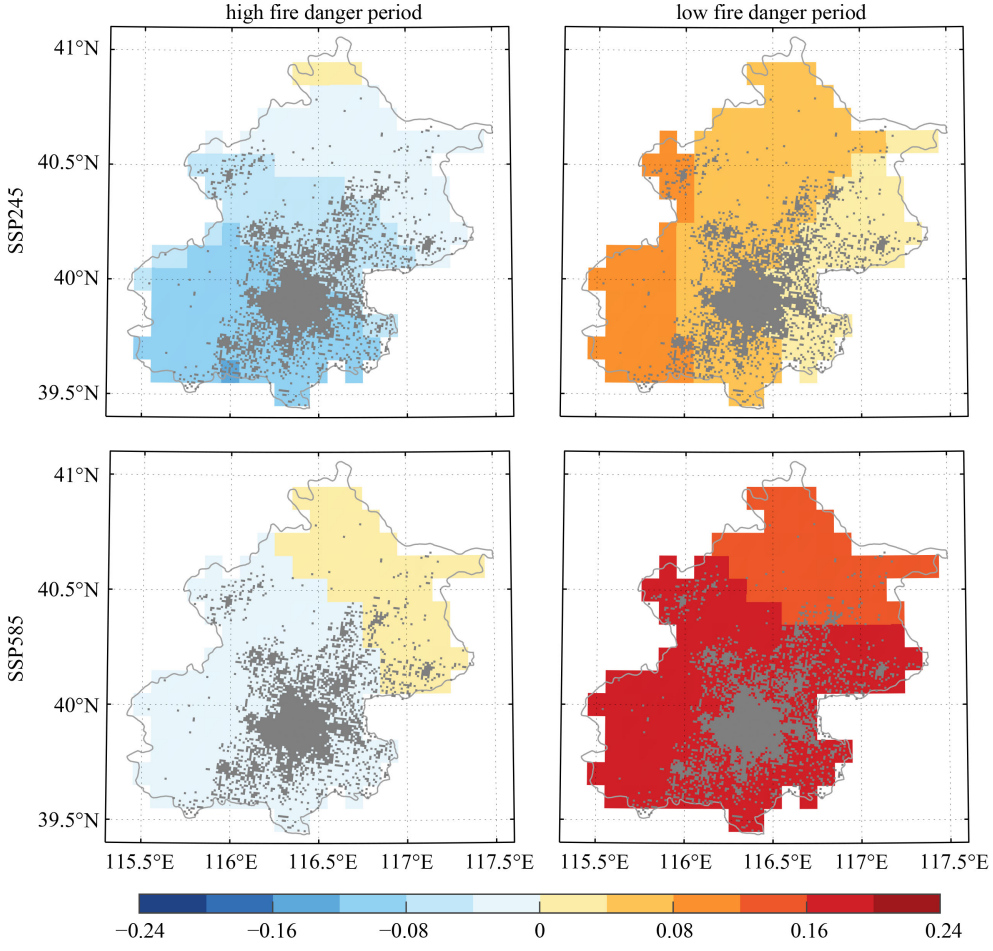

Fig. 6 Spatial patterns of FWI trends in Beijing during 2021−2100 (units: $(10\ yr)^{-1}$; gray dots represent urban areas).

−0.05/(10 yr), while a small portion of the north-west showed a trend of increasing fire danger, approximately 0.05/(10 yr). Most land was covered by forests, while there were a few spots where fire danger was increasing. The overall fire danger was decreasing, which was suitable for the growth of forest vegetation. During the low fire danger period, the south-western forest region showed the most obvious trend of a rising FWI, reaching 0.15/(10 yr), which posed a significant threat to local forest vegetation growth. Then, the fire danger trend of the northern forest increased at a rate of 0.1/(10 yr), which harmed the surrounding vegetation and severely threatened the forest in northern Beijing to serve as an ecological conservation function area. Finally, the forest fire danger in the north-east reached a higher rate of 0.5/(10 yr), which, despite the slight increase, still poses some risk to the local ecological environment.

In the context of the high emission scenario (SSP585), the spatial pattern of the FWI in Beijing during the high fire danger period of 2021−2100 showed an increasing trend in the north-east and a decreasing trend in the southern parts. However, the FWI in Beijing tended to rise during the low fire danger period. In detail, during the high fire danger period, the FWI of southern Beijing had a decreasing trend of approximately −0.05/(10 yr). The FWI in the north-eastern parts was on the rise at 0.05/(10 yr), and the overall trend was not particularly large. In southern Beijing, there was a major trend of the FWI with a growth rate of 0.2/(10 yr) or higher during the low fire danger period. This trend may seriously affect the forest vegetation in the western and southern regions, restricting their growth. The north-east had a significantly slower rate of FWI growth than other regions, topping at 0.15/(10 yr). The forest in northern Beijing could be threatened by severe climatic circumstances under the high-emission scenario, and in extreme cases, it might lose its role as an ecological conservation area.

The findings mentioned above suggested that compared with SSP245, the Beijing FWI under SSP585 showed an increasing trend, both in the high and low fire danger periods. In contrast to SSP585, in which the Beijing FWI displayed a “northeast-central to southwest” pattern throughout the high/low fire danger period, SSP245 displayed a “north–south” pattern during the high fire danger period and an “east–west” pattern during the low fire danger period. The magnitude of discrepancy between the FWI trends in the observation and simulation data may be caused by the model’s inherent systematic error.

To assess the similarities and differences in the FWI under different future stages, we examined the characteristics of Beijing FWI variations under medium-term and long-term climate projections. During the medium-term climate projection period (2021−2050), the SSP245 scenario depicted an anti-phase spatial pattern in the high fire danger period, with an increasing trend in the north-east and a decreasing trend in the western regions (Fig. 7(a)). The western parts had the highest decreasing FWI rates, up to −0.15/(10 yr). Compared to the reference period of 1991−2020, the percentage increase in the FWI in most areas of Beijing could be nearly 10%. It is noted that both trends and increase rates were based on the results of model simulations. Although the model could reproduce spatial features in observations to some extent, there were some errors between simulations and observations. This may lead to simulations in which the trend decreased, but the rate increased. This situation was also likely to result from the impact of an extreme FWI in specific years in 2021−2050, which caused an increase in its mean value relative to the base period (1991−2020) in the MME of CMIP6 models. Beijing exhibited a growing trend during the low fire

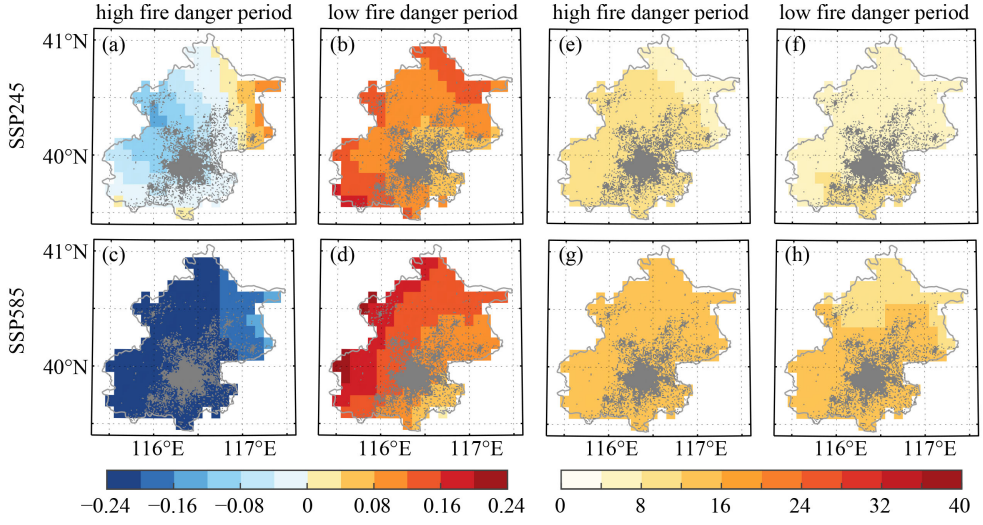

Fig. 7 Spatial patterns of FWI trends (a–d; units: (10 yr)$^{-1}$) and percentage of increase (e–h; units: %; relative to 1991–2020 in CMIP6 models) of FWI in Beijing for the medium-term projection period (2021−2050) under the SSP245 and SSP585 scenarios (gray dots represent urban areas).

danger period (Fig. 7(b)), with the north-eastern and north-western parts of the city exhibiting the most significant increasing trend, reaching a rate of 0.20/(10 yr), which may be a factor in the danger of forest fires. Meanwhile, compared to the reference period during 1991−2020, a few areas in the south had a percentage increase of more than 10%, while the percentage growth in the majority of Beijing reached over 7%. During the high fire danger period from 2070 to 2100, the SSP245 scenario depicted an overall declining trend of the FWI (Fig. 7(c)), with the falling rate exceeding −0.25/(10 yr) in most areas and being over −0.2/(10 yr) in some areas of the north-east. Compared to the reference period during 1991−2020, the average FWI growth percentage for most of Beijing could be close to 15%. It should be emphasized that the increasing rate and trend results were based on the model simulations. Similarly, this is most likely consistent with the FWI variations in SSP245 during the high fire danger period. There were some errors between the simulations and observations. There was also an impact of an extreme FWI in specific years in 2021−2050, which caused an increase in its mean value relative to the base period (1991−2020) in the MME of the CMIP6 models. In the SSP585 scenario, the FWI generally increased from the south-east to the north-west during the low fire danger period (Fig. 7(d)). Notably, there was a higher probability that forests in the west would experience fire danger. Compared to the reference period during 1991−2020, the percentage increase exceeded 15% in most areas of Beijing, and only a few areas in the north had a percentage increase of 10%.

These findings indicated that in both SSP245 and SSP585, the trends of the FWI increased for the low fire danger period and decreased for the high fire danger period during 2021−2050. In both high and low fire danger periods, the trend of the FWI for SSP585 was more substantial than that of SSP245. Moreover, the increasing trend for the FWI in SSP585 was greater and less in the high and low fire danger periods, respectively. Different scenarios exhibited an increase in the FWI relative to the reference period for both high and low fire danger periods, but the increase was more remarkable for SSP585 than SSP245.

During 2071−2100, Figure 8(a) shows a widespread increase in the high fire danger period under the SSP245 scenario. The spatial pattern gradually increased from south-west to north-east, with a maximum of more than 0.25/(10 yr) in the north-east. The low fire danger period also showed a widespread increase (Fig. 8(b)). However, its spatial pattern differed from that of the high fire danger period, with a gradual increase from north-west to south-east and a maximum of more than 0.25/(10 yr) in the south-east. Compared to the reference period during 1991−2020, the percentage increase in the low fire danger period was, on average, more prominent than that in the high fire danger periods. The possibility of urban forest fires was seriously higher in this situation.

From 2071 to 2100, the SSP585 scenario showed a widespread and consistent decreasing trend in high fire danger of more than −0.25/(10 yr), while the low fire danger period was the opposite, showing a widespread and consistent increasing trend of more than 0.25/(10 yr). Similarly, compared to the reference period from 1991−2020, the percentage increase in the high fire danger period was approximately 20% or more. However, the percentage increase in the low fire danger period averaged over 45% or more. In particular, these results in SSP585 during the high fire danger period were compatible with the FWI variations in SSP245 during the high fire danger period. There was a discrepancy error between simulations and observations. There was also an

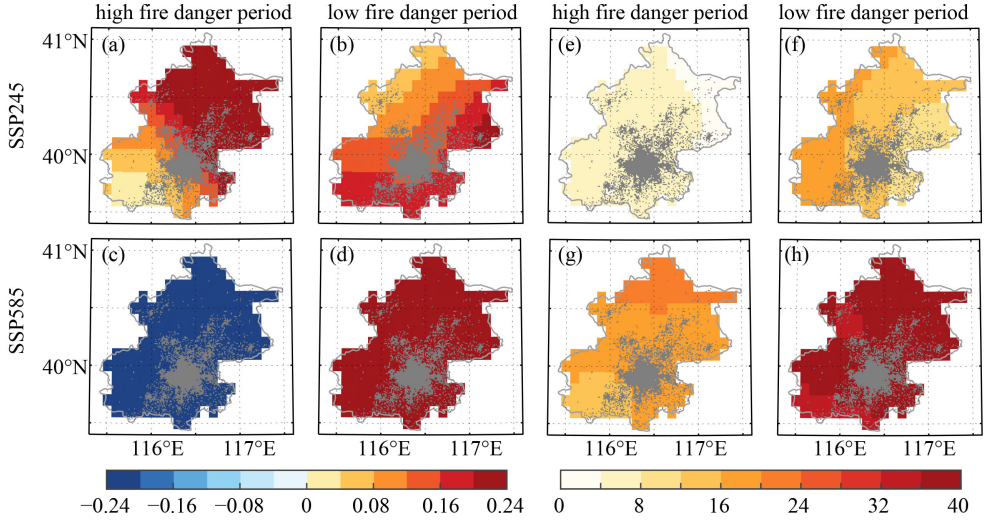

Fig. 8 Spatial patterns of FWI trends (a−d; units: $(10\ yr)^{-1}$) and percentage of increase (e−h; units: %; relative to 1991–2020 in CMIP6 models) of FWI in Beijing for long-term projections (2071−2100) under SSP-245 and SSP-585 scenarios (gray dots represent urban areas).

Table 2 Regional average FWI trends (units: $(10\ yr)^{-1}$) for different fire danger periods and SSP scenarios during 2021–2050 and 2071–2100

Scenario	Period	High fire danger period	Low fire danger period
SSP245	2021–2050	−0.0316	0.1084
	2071–2100	0.2113	0.1348
SSP585	2021–2050	−0.2709	0.1324
	2071–2100	−0.3157	0.3916

extreme FWI in particular years in 2021–2050, which increased its mean value in MME of CMIP6 models relative to the base period (1991–2020). Meanwhile, Table 2 depicts regional average FWI trends for different fire danger periods and SSP scenarios during 2021–2050 and 2071–2100. We found that both in 2021–2050 and 2071–2100, the regional average FWI trends were dominated by increase/decrease during low/high fire danger periods.

The analyses mentioned above suggested that the other three situations had a substantial increasing trend from 2071 to 2100, except for SSP585, which had a decreasing trend in the FWI during the high fire danger period. However, the spatial patterns of these three situations were inconsistent. Different SSP scenarios showed an increase in the FWI relative to the reference period for both high and low fire danger periods, but the increase was more significant for SSP585 than SSP245, with the most substantial percentage increase occurring at the end of the 21st century for the low fire danger period. Therefore, due to the significant variations in the FWI, we must focus on urban fire danger during the low fire danger period.

4 Discussion

In high-density forest areas, lower fire danger may lessen the burden on fire rescue services, harm to the local plant ecology, and aerosol pollution (Baranovskiy et al., 2023; Tian et al., 2023; Weeks et al., 2023). However, increased fire risks could affect ecology, vegetation phenology, biodiversity, and seriously harm ecological reserves, obstruct human tourism, and food production, etc. (Adámek et al., 2015; Weeks et al., 2023). Meanwhile, air pollutants from vegetation burning may enter the city, and hence pollute the environment and threaten human health (Slezakova et al., 2013). Importantly, the capacity of the forest to sequester carbon, and the targets of "peak carbon dioxide emissions" and "carbon neutrality," may be affected by the destruction of forest vegetation by fire danger, such as in mega-cities like Beijing (Hurteau and North, 2010; Zhu and Zhu, 2021).

Notably, although numerous studies have shown a strong positive correlation between the FWI and fire conditions, the FWI measures the level of fire danger based on local meteorological conditions and does not reflect the frequency and areas of local fires. It reflects a risk indicator for fire through comprehensive consideration of meteorological factors. Meanwhile, we only used one output from each model. The contamination of climate internal variability on research results may not be completely removed with the multi-model ensemble mean method. Large sample ensemble results for one climate model may represent another method of weakening contamination caused by climate internal variability on the research results. Therefore, we would prefer to use a large sample ensemble mean for one model to reflect the characteristics of the FWI in the future. Moreover, we need to apply downscaling techniques to drive the FWI to a finer grid in future studies so that government officials may precisely find high fire hazard regions and implement efficient preventive actions to effectively improve local government management of local fire dangers.

5 Conclusions

The above-mentioned results demonstrated that the FWI had a intra-annual cycle throughout the year, with a high fire danger period in spring (April and May) and a low fire danger period in summer (July and August). During the high fire danger period, the FWI in Beijing showed a spatial pattern of a "decreasing trend in the northwest and increasing trend in the southeast". During the low fire danger period, the FWI for the entire Beijing region revealed a trend of significant large-scale increase. The primary meteorological factors influencing FWI trends differed between different fire danger periods. In the high fire danger period, the trend variations of the FWI in most of Beijing were influenced by precipitation, and some areas in the south were influenced by the RH_{min}. In the low fire danger period, the FWI trend variations in most areas were mainly influenced by wind speed variations.

During 2021–2100, the Beijing FWI under SSP585 showed an increasing trend, both in the high and low fire danger periods, compared with SSP245. In contrast to SSP585, in which the Beijing FWI displayed a "northeast-southwest" pattern throughout the high/low fire danger period, SSP245 displayed a "north–south" pattern during the high fire danger period and an "east–west" pattern during the low fire danger period. In both SSP245 and SSP585, the trends of the FWI increased for the low fire danger period and decreased for the high fire danger period during 2021–2050. In both high and low fire danger periods, the trend of the FWI for SSP585 was more substantial than that of SSP245. The other three situations had a substantial increasing trend from 2071 to 2100, except for SSP585, which had a decreasing trend in the FWI during the high fire danger period.

Acknowledgments This research was funded by the National Natural Science Foundation of China (Grant Nos. 42305055, 42171030 and 41901017), the Science and Technology Project of Beijing Meteorological Service (No. BMBKJ202302001), the Key Project of Beijing Academy of Emergency Management Science and Technology (No. Y2023046) and Open Foundation of Key Laboratory of Land Surface Pattern and Simulation, Chinese Academy of Sciences. We thank the Beijing Meteorological Information Center, Beijing Meteorological Service for the daily observational meteorological data.

Author Contributions Conceptualization, M.B., W.D. and Z.H.; methodology, M.B. and W.D.; software, M.B., L.Z. and P.X.; formal analysis, M.B., W.D., Z.H. and P.X.; writing—original draft preparation, M.B., W.D., Z.H., L.Z. and P.X.; writing—review and editing, W.D and Z.H. All authors have read and agreed to the published version of the manuscript.

Competing interests The authors declare that they have no competing interests.

References

Adámek M, Bobek P, Hadincova V, Wild J, Kopecky M (2015). Forest fires within a temperate landscape: a decadal and millennial perspective from a sandstone region in Central Europe. For Ecol Manage, 336: 81–90

Amiro B D, Logan K A, Wotton B M, Flannigan M D, Todd J B, Stocks B J, Martell D L (2004). Fire weather index system components for large fires in the Canadian boreal forest. Int J Wildland Fire, 13(4): 391–400

Baranovskiy N V, Vyatkina V A, Chernyshov A M (2023). Deterministic-probabilistic prediction of forest fires from lightning activity taking into account aerosol emissions. Atmosphere (Basel), 14(1): 29

Cai D J, Abram N J, Sharples J J, Perkins-Kirkpatrick S E (2022). Increasing intensity and frequency of cold fronts contributed to Australia's 2019–2020 Black Summer fire disaster. Environ Res Lett, 17(9): 094044

Cheng L L, Zhang Y, Sun H Y (2020). Vegetation cover change and relative contributions of associated driving factors in the ecological conservation and development zone of Beijing, China. Pol J Environ Stud, 29(1): 53–65

de Groot W J, Landry R, Kurz W A, Anderson K R, Englefield P, Fraser R H, Hall R J, Banfield E, Raymond D A, Decker V, Lynham T J, Pritchard J M (2007). Estimating direct carbon emissions from Canadian wildland fires. Int J Wildland Fire, 16(5): 593–606

de Sousa J A P, do Nascimento Lope E R, Duarte M L, Ewbank H, Lourenço R W (2022). Forest fire risk indicator (FFRI) based on geoprocessing and multicriteria analysis. Nat Hazards, 114(2): 2311–2330

Ding Y H, Sun Y, Wang Z Y, Zhu Y X, Song Y F (2009). Inter-decadal variation of the summer precipitation in China and its association with decreasing Asian summer monsoon Part II: possible causes. Int J Climatol, 29(13): 1926–1944

Ding Y H, Wang Z Y, Sun Y (2008). Inter-decadal variation of the summer precipitation in east China and its association with decreasing Asian summer monsoon. Part I: observed evidences. Int J Climatol, 28(9): 1139–1161

Esperson-Rodriguez M, Tjoelker M G, Lenoir J, Baumgartner J B, Beaumont L J, Nipperess D A, Power S A, Richard B, Rymer P D, Gallagher R V (2022). Climate change increases global risk to urban forests. Nat Clim Change, 12(10): 950–955

Flannigan M D, Krawchuk M A, de Groot W J, Wotton B M, Gowman L M (2009). Implications of changing climate for global wildland fire. Int J Wildland Fire, 18(5): 483–507

Guidolotti G, Calfapietra C, Pallozzi E, De Simoni G, Esposito R, Mattioni M, Nicolini G, Matteucci G, Brugnoli E (2017). Promoting the potential of flux-measuring stations in urban parks: an innovative case study in Naples, Italy. Agric For Meteorol, 233: 153–162

Hardiman B S, Wang J A, Hutyra L R, Gately C K, Getson J M, Friedl M A (2017). Accounting for urban biogenic fluxes in regional carbon budgets. Sci Total Environ, 592: 366–372

Hurteau M D, North M (2010). Carbon recovery rates following different wildfire risk mitigation treatments. For Ecol Manage, 260(5): 930–937

Ibsen P C, Borowy D, Dell T, Greydanus H, Gupta N, Hondula D M, Meixner T, Santelmann M V, Shiflett S A, Sukop M C, Swan C M, Talal M L, Valencia M, Wright M K, Jenerette G D (2021). Greater aridity increases the magnitude of urban nighttime vegetation-derived air cooling. Environ Res Lett, 16(3): 034011

Jain P, Castellanos-Acuna D, Coogan S C P, Abatzoglou J T, Flannigan M D (2022). Observed increases in extreme fire weather driven by atmospheric humidity and temperature. Nat Clim Chang, 12(1): 63–70

Jia P P, Zhuang D F, Wang Y (2017). Impacts of temperature and precipitation on the spatiotemporal distribution of water resources in Chinese mega cities: the case of Beijing. J Water Clim Chang, 8(4): 593–612

Jolly W M, Cochrane M A, Freeborn P H, Holden Z A, Brown T J, Williamson G J, Bowman D M J S (2015). Climate-induced variations in global wildfire danger from 1979 to 2013. Nat Commun, 6(1): 7537

Justino F, de Melo A S, Setzer A, Sismanoglu R, Sediyama G C, Ribeiro G A, Machado J P, Sterl A (2011). Greenhouse gas induced changes in the fire risk in Brazil in ECHAM5/MPI-OM coupled climate model. Clim Change, 106(2): 285–302

Kelly L T, Giljohann K M, Duane A, Aquilue N, Archibald S, Batllori E, Bennett A F, Buckland S T, Canelles Q, Clarke M F, Fortin M J, Hermoso V, Herrando S, Keane R E, Lake F K, McCarthy M A, Morán-Ordóñez A, Parr C L, Pausas J G, Penman T D, Regos A, Rumpff L, Santos J L, Smith A L, Syphard A D, Tingley M W, Brotons L (2020). Fire and biodiversity in the Anthropocene. Science, 370(6519): eabb0355

Kloster S, Mahowald N M, Randerson J T, Lawrence P J (2012). The impacts of climate, land use, and demography on fires during the 21st century simulated by CLM-CN. Biogeosciences, 9(1): 509–525

McDowell N G, Allen C D (2015). Darcy's law predicts widespread forest mortality under climate warming. Nat Clim Chang, 5(7): 669–672

Nolan R H, Boer M M, Collins L, Resco de Dios V R, Clarke H,

Jenkins M, Kenny B, Bradstock R A (2020). Causes and consequences of eastern Australia's 2019–20 season of mega-fires. Glob Change Biol, 26(3): 1039–1041

O'Neill B C, Tebaldi C, van Vuuren D P, Eyring V, Friedlingstein P, Hurtt G, Knutti R, Kriegler E, Lamarque J F, Lowe J, Meehl G A, Moss R, Riahi K, Sanderson B M (2016). The Scenario Model Intercomparison Project (ScenarioMIP) for CMIP6. Geosci Model Dev, 9(9): 3461–3482

Pataki D E, Alberti M, Cadenasso M L, Felson A J, McDonnell M J, Pincetl S, Pouyat R V, Setala H, Whitlow T H (2021). The benefits and limits of urban tree planting for environmental and human health. Front Ecol Evol, 9: 603757

Riahi K, van Vuuren D P, Kriegler E, Edmonds J, O'Neill B C, Fujimori S, Bauer N, Calvin K, Dellink R, Fricko O, Lutz W, Popp A, Cuaresma J C, Kc S, Leimbach M, Jiang L, Kram T, Rao S, Emmerling J, Ebi K, Hasegawa T, Havlik P, Humpenöder F, Da Silva L A, Smith S, Stehfest E, Bosetti V, Eom J, Gernaat D, Masui T, Rogelj J, Strefler J, Drouet L, Krey V, Luderer G, Harmsen M, Takahashi K, Baumstark L, Doelman J C, Kainuma M, Klimont Z, Marangoni G, Lotze-Campen H, Obersteiner M, Tabeau A, Tavoni M (2017). The shared socioeconomic pathways and their energy, land use, and greenhouse gas emissions implications: an overview. Glob Environ Change, 42: 153–168

Richards D R, Belcher R N, Carrasco L R, Edwards P J, Fatichi S, Hamel P, Masoudi M, McDonnell M J, Peleg N, Stanley M C (2022). Global variation in contributions to human well-being from urban vegetation ecosystem services. One Earth, 5(5): 522–533

Slezakova K, Morais S, Pereira M D (2013). Forest fires in Northern region of Portugal: impact on PM levels. Atmos Res, 127: 148–153

Spracklen D V, Mickley L J, Logan J A, Hudman R C, Yevich R, Flannigan M D, Westerling A L (2009). Impacts of climate change from 2000 to 2050 on wildfire activity and carbonaceous aerosol concentrations in the western United States. J Geophys Res, 114: D20301

Squire D T, Richardson D, Risbey J S, Black A S, Kitsios V, Matear R J, Monselesan D, Moore T S, Tozer C R (2021). Likelihood of unprecedented drought and fire weather during Australia's 2019 megafires. NPJ Clim Atmos Sci, 4(1): 64

Taylor K E, Stouffer R J, Meehl G A (2012). An overview of CMIP5 and the experiment design. Bull Am Meteorol Soc, 93(4): 485–498

Tian X M, Tang C L, Wu X, Yang J, Zhao F M, Liu D (2023). The global spatial-temporal distribution and EOF analysis of AOD based on MODIS data during 2003–2021. Atmos Environ, 302: 119722

Tian X R, McRae D J, Jin J Z, Shu L F, Zhao F J, Wang M Y (2011). Wildfires and the Canadian forest fire weather index system for the Daxing'anling region of China. Int J Wildland Fire, 20(8): 963–973

Tian X R, Shu L F, Wang M Y (2006). Study on assessment of Beijing forest fire danger. Fire Safety Sci, 15(3): 150–158 (in Chinese)

Wagner C E V (1987). Development and structure of the Canadian Forest Fire Weather Index System. Canadian Forestry Service, Forestry Technical Report 35: 1–48

Ward M, Tulloch A I T, Radford J Q, Williams B A, Reside A E, Macdonald S L, Mayfield H J, Maron M, Possingham H P, Vine S J, O'Connor J L, Massingham E J, Greenville A C, Woinarski J C Z, Garnett S T, Lintermans M, Scheele B C, Carwardine J, Nimmo D G, Lindenmayer D B, Kooyman R M, Simmonds J S, Sonter L J, Watson J E M (2020). Impact of 2019–2020 mega-fires on Australian fauna habitat. Nat Ecol Evol, 4(10): 1321–1326

Weeks J, Miller J E D, Steel Z L, Batzer E E, Safford H D (2023). High-severity fire drives persistent floristic homogenization in human-altered forests. Ecosphere, 14(2): e4409

Wei S Y, Chen Q J, Wu W B, Ma J (2021). Quantifying the indirect effects of urbanization on urban vegetation carbon uptake in the megacity of Shanghai, China. Environ Res Lett, 16(6): 064088

Xie G D, Li W H, Xiao Y, Zhang B A, Lu C X, An K, Wang J X, Xu K, Wang J Z (2010). Forest ecosystem services and their values in Beijing. Chin Geogr Sci, 20(1): 51–58

Ying L X, Shen Z H, Guan P G, Cao J, Luo C F, Peng X Z, Cheng H J (2022). Impacts of the Western Pacific and Indian Ocean warm pools on wildfires in Yunnan, Southwest China: spatial patterns with interannual and intraannual variations. Geophys Res Lett, 49(11): e2022GL098797

Zhang Y F, Jia D M, Zhang H Y, Tan J, Song S Y, Sun R F (2011). Spatial structure of valley economic development in the mountainous areas in Beijing. J Geogr Sci, 21(2): 331–345

Zhu Z, Zhu X (2021). Study on spatiotemporal characteristic and mechanism of forest loss in urban agglomeration in the middle reaches of the Yangtze River. Forests, 12(9): 1242

Zou Y F, Rasch P J, Wang H L, Xie Z W, Zhang R D (2021). Increasing large wildfires over the western United States linked to diminishing sea ice in the Arctic. Nat Commun, 12(1): 6048